DETERMINISTIC CRAMÉR-RAO BOUNDS FOR STRICT SENSE NON-CIRCULAR SOURCES

Florian Römer and Martin Haardt

Ilmenau University of Technology, Communications Research Laboratory
P.O. Box 100565, D-98684 Ilmenau, Germany
Phone: +49 (3677) 69-2613
florian.roemer@ieee.org, martin.haardt@tu-ilmenau.de

Workshop Topic: Space-time processing

ABSTRACT

In this contribution, the Cramér-Rao Bound (CRB) for direction of arrival (DOA) estimation in presence of strict sense non-circular sources is given. These types of sources are used in numerous practical systems and enhancements to parameter estimation methods exploiting non-circularity have received considerable attention recently [5, 12, 1, 8]. While closed-form expressions for the CRB for other types of non-circularity are known [3], the closed-form expression for the CRB for this data model is not available in the literature to date. After providing the closed-form expression, some interesting special cases are discussed. The cases where strict sense non-circularity does not provide any gain over generic source constellations are stated. Moreover, it is demonstrated that under certain conditions the joint CRB may decouple into independent groups. It is also shown that the number of sources which can be estimated jointly is increased. The analytical results are supported by computer simulations which show the Cramér-Rao Bounds along with the corresponding versions of the Unitary ESPRIT algorithm.

1. INTRODUCTION

Estimating the directions of arrival of several planer wavefronts impinging on an antenna array is a task required for a variety of applications, including channel modeling, radar, communications, sonar, and seismology. In recent publications it was shown how existing parameter estimation methods can be improved if the source symbols fulfill a condition we term strict sense non-circularity, e.g., the NC Unitary ESPRIT algorithm discussed in [5], extensions to standard ESPRIT given in [12], or improved versions of MUSIC proposed in [1, 8]. In this contribution, the deterministic Cramér-Rao Bound for strict sense non-circular sources is discussed. For this data model, a closed-form expression for the CRB has not been derived before.

This paper is organized as follows. First, the data model is introduced and weak sense as well as strict sense non-circularity is defined. Then the Cramér-Rao Bound for strict sense non-circular sources is shown. The main steps of its derivation are outlined. In the next part, interesting special cases of the CRB are discussed. In particular, the cases where the restriction to non-circular source constellations does not provide any gain are outlined. In the case of two or more sources with small angular separation, the achievable gains are shown. The fact that the non-circular data model facilitates the estimation of twice the number of sources compared to generic source constellations is also highlighted. Finally, some numerical results demonstrate the Cramér-Rao Bounds along with the performance of the corresponding versions of the Unitary ESPRIT algorithm [4, 5].

2. DATA MODEL

The following simplified model is used for the description of the proposed methods: We assume that the measurements represent a superposition of d specular components resulting from narrowband sources located in the far field of the antenna array. We can therefore write the measurement matrix $\boldsymbol{X} \in \mathbb{C}^{M \times N}$ containing samples from the M antenna elements at N subsequent time instances as

$$\boldsymbol{X} = \boldsymbol{A} \cdot \boldsymbol{S} + \boldsymbol{N}, \tag{1}$$

where $\boldsymbol{A} \in \mathbb{C}^{M \times d}$ denotes the array steering matrix which consists of d array steering vectors $\boldsymbol{a}_1, \ldots, \boldsymbol{a}_d$, $\boldsymbol{S} \in \mathbb{C}^{d \times N}$ containes N subsequent symbols from the d users, and $\boldsymbol{N} \in \mathbb{C}^{M \times N}$ represents samples of the additive noise component which are assumed to be complex Gaussian distributed with zero mean and variance σ^2 and mutually uncorrelated.

Strict sense non-circularity can be defined through the non-circularity rate [3] which we denote by ϑ. For every complex random variable Z with mean zero, the non-circularity rate is given by

$$\vartheta = \frac{\mathrm{E}\{Z^2\}}{\mathrm{E}\{|Z|^2\}}. \tag{2}$$

A random variable for which ϑ is equal to zero is termed circularly symmetric. Conversely, the case where $|\vartheta| > 0$ is referred to as weak sense non-circularity. It can be shown that for any zero mean complex random variable Z the non-circularity rate fulfills $|\vartheta| \leq 1$ with equality if and only if the real part and the imaginary part of Z are linearly dependent, i.e., $c_1 \cdot \mathrm{Re}\{Z\} = c_2 \cdot \mathrm{Im}\{Z\}$ for constants $c_1, c_2 \in \mathbb{R}$. This particular case is referred to as strict sense non-circularity, i.e., a random variable Z is strict sense non-circular if and only if its non-circularity rate ϑ satisfies $|\vartheta| = 1$.

The Cramér-Rao Bound for weak sense non-circular sources has been derived in [3]. However, this bound does not apply to the strict sense case since in the weak sense case the real part and the imaginary part can be treated as different random variables. This is not true in the strict sense case due to the linear dependence.

In the context of direction of arrival estimation, the requirement for strict sense non-circular sources is that for each source the symbols that are received are located on a line in the I/Q diagram. Such a scenario is, for example, found when the sources transmit real-valued data but may have different transmit delays and therefore their phase angles φ_i, $i = 1, 2, \ldots, d$ at the receiver can be different. The strict sense non-circularity constraint is incorporated into the data model in the following fashion

$$\boldsymbol{X} = \boldsymbol{A} \cdot \boldsymbol{\Psi} \cdot \boldsymbol{S}_0 + \boldsymbol{N}, \tag{3}$$

where now the matrix $\boldsymbol{S}_0 \in \mathbb{R}^{d\times N}$ contains real-valued symbols from d sources at N time instances and the matrix $\boldsymbol{\Psi}$ is constructed from the phases φ_i, $i = 1, 2, \ldots, d$ in the following fashion

$$\boldsymbol{\Psi} = \operatorname{diag}\left\{\left[e^{j\varphi_1},\ e^{j\varphi_2},\ \ldots, e^{j\varphi_d}\right]\right\}. \tag{4}$$

3. CRAMÉR-RAO BOUND

The Cramér-Rao Bound represents a lower limit on the variance of any unbiased estimator [2, 6] and is therefore a valuable tool to benchmark the performance of parameter estimation methods. In particular, the Cramér-Rao inequality states that the covariance matrix of any unbiased estimator $\hat{\boldsymbol{\theta}}(\boldsymbol{x})$ aiming to compute estimates for a parameter vector $\boldsymbol{\theta}$ from an observation vector $\boldsymbol{x}$ satisfies

$$\operatorname{COV}\left\{\hat{\boldsymbol{\theta}}(\boldsymbol{x})\right\} \geq \boldsymbol{C} \tag{5}$$

where $\boldsymbol{C}$denotes the corresponding CRB matrix and the inequality is to be understood in the following sense

$$\boldsymbol{A} \geq \boldsymbol{B} \ \Leftrightarrow\ \boldsymbol{A} - \boldsymbol{B} \text{ is positive semi-definite.} \tag{6}$$

The CRB matrix is computed from the inverse of the Fisher information matrix (see below).

Closed-form expressions for the Cramér-Rao Bound have been derived under various assumptions. The most prominent among these are the deterministic CRB (assuming that the symbols are arbitrary complex numbers which are constant but unknown at the receiver) [9] and the stochastic CRB (assuming that the symbols represent samples from a complex random process with known covariance matrix) [10]. The latter was also derived for weak sense non-circular sources in [3]. However, as it has been mentioned above, this CRB is not applicable in the strict sense non-circular case since there we cannot assume the real part and the imaginary part of the symbols to be independent random variables anymore.

In this paper, we consider the deterministic case, i.e., we model the symbols to be constant but unknown random variables. In the case of arbitrary (i.e., not neccessarily non-circular) constellations, the set of parameters that need to be considered is then given by:

- The azimuth angles $\boldsymbol{\theta} \in \mathbb{R}^d$.
- The real part and the imaginary part of the $d \cdot N$ symbols $\boldsymbol{s} = \operatorname{vec}\{\boldsymbol{S}\} \in \mathbb{C}^{d\cdot N}$.
- The standard deviation of the noise σ,

constituting a total of $(2N + 1)d + 1$ paremters. For the 2-D case (i.e., joint azimuth and elevation estimation) we additionally have the d elevation angles $\boldsymbol{\alpha} \in \mathbb{R}^d$. For simplicity, we present the 1-D case first. The generalization to the 2-D case is shown in Section 4.

The CRB matrix derived under these assumptions is denoted by $\boldsymbol{C}$. Its closed-form expression is given by [9]

$$\begin{aligned}
\boldsymbol{C} &= \frac{\sigma^2}{2N} \cdot \operatorname{Re}\left\{\left(\boldsymbol{D}^H \cdot \boldsymbol{\Pi}_{\boldsymbol{A}}^{\perp} \cdot \boldsymbol{D}\right) \odot \hat{\boldsymbol{R}}_S\right\}^{-1} \qquad (7)\\
\boldsymbol{\Pi}_{\boldsymbol{A}}^{\perp} &= \boldsymbol{I}_M - \boldsymbol{A} \cdot \left(\boldsymbol{A}^H \cdot \boldsymbol{A}\right)^{-1} \cdot \boldsymbol{A}^H\\
\hat{\boldsymbol{R}}_S &= \boldsymbol{\Psi}^* \cdot \hat{\boldsymbol{R}}_{S,0} \cdot \boldsymbol{\Psi}, \quad \hat{\boldsymbol{R}}_{S,0} = \frac{1}{N}\boldsymbol{S}_0\boldsymbol{S}_0^T\\
\boldsymbol{D} &= \left[\frac{\partial \boldsymbol{a}_1}{\partial \theta_1},\ \frac{\partial \boldsymbol{a}_2}{\partial \theta_2},\ ,\ldots,\ \frac{\partial \boldsymbol{a}_d}{\partial \theta_d}\right].
\end{aligned}$$

In contrast to this approach, for strict sense non-circular sources the set of parameters is given by:

- The azimuth angles $\boldsymbol{\theta} \in \mathbb{R}^d$.
- The $d \cdot N$ real-valued symbols $\boldsymbol{s}_0 = \operatorname{vec}\{\boldsymbol{S}_0\} \in \mathbb{R}^{d\cdot N}$.
- The d phase angles $\boldsymbol{\varphi} \in \mathbb{R}^d$.
- The standard deviation of the noise σ.

As we can see the number of parameters is now equal to $(2+N)d+1$. Under these conditions, it can be shown that the expression for the deterministic CRB is given by equation (8) (see below), where the matrices $\boldsymbol{G}_n$, $\boldsymbol{H}_n$, $n = 0, 1, 2$ are defined as

$$\begin{aligned}
\boldsymbol{G}_0 &= \operatorname{Re}\left\{\boldsymbol{\Psi}^* \cdot \boldsymbol{A}^H \cdot \boldsymbol{A} \cdot \boldsymbol{\Psi}\right\}\\
\boldsymbol{H}_0 &= \operatorname{Im}\left\{\boldsymbol{\Psi}^* \cdot \boldsymbol{A}^H \cdot \boldsymbol{A} \cdot \boldsymbol{\Psi}\right\}\\
\boldsymbol{G}_1 &= \operatorname{Re}\left\{\boldsymbol{\Psi}^* \cdot \boldsymbol{D}^H \cdot \boldsymbol{A} \cdot \boldsymbol{\Psi}\right\}\\
\boldsymbol{H}_1 &= \operatorname{Im}\left\{\boldsymbol{\Psi}^* \cdot \boldsymbol{D}^H \cdot \boldsymbol{A} \cdot \boldsymbol{\Psi}\right\}\\
\boldsymbol{G}_2 &= \operatorname{Re}\left\{\boldsymbol{\Psi}^* \cdot \boldsymbol{D}^H \cdot \boldsymbol{D} \cdot \boldsymbol{\Psi}\right\}\\
\boldsymbol{H}_2 &= \operatorname{Im}\left\{\boldsymbol{\Psi}^* \cdot \boldsymbol{D}^H \cdot \boldsymbol{D} \cdot \boldsymbol{\Psi}\right\}
\end{aligned} \tag{9}$$

and the remaining terms are defined in (7). The derivation of (8) can be carried out in analogy to the one presented in [9]. The main steps are:

- Establishing the probability density function (pdf) of the measurements. Since the parameters are assumed constant, the measurement samples are complex Gaussian distributed with mean given by the measurement model.
- Computing the log-likelihood function (LLF) as the logarithm of the pdf. It is a function depending on the current realization of the measurement process as well as all the parameters which are to be estimated.
- From the LLF we can obtain the score-function $\boldsymbol{q}$ which is a vector containing the partial derivatives of the LLF with respect to all the parameters. It is important to include not only the parameters which we would like to estimate but also the nuisance parameters.
- The Fisher information matrix $\boldsymbol{J}$ is then given by $\mathrm{E}\{\boldsymbol{q}\boldsymbol{q}^T\}$ where the expectation is carried out with respect to the noise.
- Finally, the CRB matrix is given by the inverse of $\boldsymbol{J}$. Since we are only interested in the variance of the direction of arrival angles, we usually only consider the block of the CRB matrix related to these paramteres.

A full version of the proof is given in [7].

4. GENERALIZATION TO THE 2-D CASE

The deterministic CRB shown in equation (7) can easily be generalized to the 2-D case (i.e., joint estimation of the azimuth angles θ and the elevation angles α) in the following way [11]

$$\begin{aligned}
\boldsymbol{C}_{2\mathrm{D}} &= \frac{\sigma^2}{2N} \cdot \operatorname{Re}\left\{\left(\boldsymbol{D}_{2\mathrm{D}}^H \cdot \boldsymbol{\Pi}_{\boldsymbol{A}}^{\perp} \cdot \boldsymbol{D}_{2\mathrm{D}}\right) \odot \hat{\boldsymbol{R}}_{S,2\mathrm{D}}\right\}^{-1}, \text{where}\\
\boldsymbol{D}_{2\mathrm{D}} &= \left[\frac{\partial \boldsymbol{a}_1}{\partial \theta_1},\ \ldots,\ \frac{\partial \boldsymbol{a}_d}{\partial \theta_d},\ \frac{\partial \boldsymbol{a}_1}{\partial \alpha_1},\ \ldots,\ \frac{\partial \boldsymbol{a}_d}{\partial \alpha_d}\right] \in \mathbb{C}^{M\times 2d} \qquad (10)\\
\hat{\boldsymbol{R}}_{S,2\mathrm{D}} &= \begin{bmatrix} 1 & 1\\ 1 & 1 \end{bmatrix} \otimes \hat{\boldsymbol{R}}_S \in \mathbb{C}^{2d\times 2d}.
\end{aligned}$$

Here $\otimes$ represents the Kronecker product operator.

In a very similar manner, the CRB for strict sense non-circular sources provided in equation (8) is generalized to the 2-D case by replacing

$$\hat{\boldsymbol{R}}_{S,0} \quad \text{by} \quad \begin{bmatrix} 1 & 1\\ 1 & 1 \end{bmatrix} \otimes \hat{\boldsymbol{R}}_{S,0} \tag{11}$$

$$\text{and} \qquad \boldsymbol{D} \quad \text{by} \quad \boldsymbol{D}_{2\mathrm{D}} \tag{12}$$

in equations (8) and (9).

$$
\begin{aligned}
\boldsymbol{C}^{(\mathrm{nc})} \;=\; & \tfrac{\sigma^2}{2N}\Big\{ \left(\boldsymbol{G}_2 - \boldsymbol{G}_1\boldsymbol{G}_0^{-1}\boldsymbol{G}_1^T\right) \odot \hat{\boldsymbol{R}}_{S,0} + \Big[\left(\boldsymbol{G}_1\boldsymbol{G}_0^{-1}\boldsymbol{H}_0\right) \odot \hat{\boldsymbol{R}}_{S,0}\Big] \Big[\left(\boldsymbol{G}_0 - \boldsymbol{H}_0^T\boldsymbol{G}_0^{-1}\boldsymbol{H}_0\right) \odot \hat{\boldsymbol{R}}_{S,0}\Big]^{-1} \\
& \cdot \Big[\left(\boldsymbol{H}_1^T - \boldsymbol{H}_0^T\boldsymbol{G}_0^{-1}\boldsymbol{G}_1^T\right) \odot \hat{\boldsymbol{R}}_{S,0}\Big] + \Big[\boldsymbol{H}_1 \odot \hat{\boldsymbol{R}}_{S,0}\Big] \cdot \Big[\boldsymbol{G}_0 \odot \hat{\boldsymbol{R}}_{S,0}\Big]^{-1} \cdot \Big[\left(\boldsymbol{H}_0^T\boldsymbol{G}_0^{-1}\boldsymbol{G}_1^T\right) \odot \hat{\boldsymbol{R}}_{S,0}\Big] \\
& + \Big[\boldsymbol{H}_1 \odot \hat{\boldsymbol{R}}_{S,0}\Big] \cdot \Big[\boldsymbol{G}_0 \odot \hat{\boldsymbol{R}}_{S,0}\Big]^{-1} \cdot \Big[\left(\boldsymbol{H}_0^T\boldsymbol{G}_0^{-1}\boldsymbol{H}_0\right) \odot \hat{\boldsymbol{R}}_{S,0}\Big] \cdot \Big[\left(\boldsymbol{G}_0 - \boldsymbol{H}_0^T\boldsymbol{G}_0^{-1}\boldsymbol{H}_0\right) \odot \hat{\boldsymbol{R}}_{S,0}\Big]^{-1} \\
& \cdot \Big[\left(\boldsymbol{H}_0^T\boldsymbol{G}_0^{-1}\boldsymbol{G}_1^T\right) \odot \hat{\boldsymbol{R}}_{S,0}\Big] - \Big[\boldsymbol{H}_1 \odot \hat{\boldsymbol{R}}_{S,0}\Big] \cdot \Big[\left(\boldsymbol{G}_0 - \boldsymbol{H}_0^T\boldsymbol{G}_0^{-1}\boldsymbol{H}_0\right) \odot \hat{\boldsymbol{R}}_{S,0}\Big]^{-1} \cdot \Big[\boldsymbol{H}_1^T \odot \hat{\boldsymbol{R}}_{S,0}\Big] \Big\}^{-1},
\end{aligned}
\tag{8}
$$

5. PROPERTIES OF THE CRB

Using the closed form expression for the CRB in (8), a number of interesting results can be shown analytically.

Full coherence: If all the d sources are coherent, i.e., the magnitude of the sample cross correlation coefficients between each pair of sources is equal to one, it can be shown that $\boldsymbol{C}^{(\mathrm{nc})} = \boldsymbol{C}$. Therefore, in this case restricting the source constellations to be non-circular does not provide any gain in terms of the estimation accuracy of any unbiased estimator.

Equal phases: The same effect is observed when the phase angles of all the sources are equal modulo π, i.e., $\varphi_i = \varphi + k_i \cdot \pi$ for $i = 1, 2, \ldots, d$, $k_i \in \mathbb{Z}$, and an arbitrary φ. This implies that the symbols received from **all** the users are constrained to **a single** line in the I/Q diagram. In this case there is also no gain from using non-circular sources since $\boldsymbol{C}^{(\mathrm{nc})} = \boldsymbol{C}$.

Single source: Finally, the case where there is only one source (i.e., $d = 1$) can be seen as a special case of both cases mentioned above. Consequently, the CRBs (which are in this case scalar) satisfy again $C^{(\mathrm{nc})} = C$ and the restriction to non-circular source constellations does not provide any gain, which is, in fact, rather surprising.

In the case where there are **two sources** it is therefore interesting to study the effect of the sample correlation coefficient $\hat{\rho}$ defined as

$$
\hat{\rho} = \frac{\frac{1}{N}\sum_{t=1}^{N} s_{0,1}(t) s_{0,2}(t)}{\sqrt{\frac{1}{N}\sum_{t=1}^{N} s_{0,1}(t)^2}\sqrt{\frac{1}{N}\sum_{t=1}^{N} s_{0,2}(t)^2}} \tag{13}
$$

and the phase separation $\Delta\varphi = \varphi_1 - \varphi_2$. For the latter, from its meaning in the complex I/Q diagram it is easily deduced that only the interval between $\Delta\varphi = 0$ and $\Delta\varphi = \pi/2$ is of interest[1]. We can then prove the following results:

- For two sources approaching in the azimuth plane, we have

$$
\begin{aligned}
&\lim_{|\theta_1 - \theta_2| \to 0} \boldsymbol{C}^{(\mathrm{nc})} = \boldsymbol{C}^{(\mathrm{nc})}_{\lim}, \text{ where} \\
&\mathrm{tr}\left\{\boldsymbol{C}^{(\mathrm{nc})}_{\lim}\right\} < \infty \Leftrightarrow \hat{\rho} < 1 \textbf{ and } \Delta\varphi > 0,
\end{aligned}
\tag{14}
$$

  where $\mathrm{tr}\{.\}$ denotes the trace of a matrix. In other words, the CRB $\boldsymbol{C}^{(\mathrm{nc})}$ reaches a finite value if the sources are not fully coherent and have a different phase. It should be noted that this results in a significant gain over the CRB $\boldsymbol{C}$ since

$$
\lim_{|\theta_1 - \theta_2| \to 0} \mathrm{tr}\{\boldsymbol{C}\} \to \infty \;\; \forall\hat{\rho}, \; \forall\Delta\varphi \tag{15}
$$

- If we have $\hat{\rho} = 0$ **and** $\Delta\varphi = \pi/2$, i.e., perfectly uncorrelated sources with maximum phase separation then the joint CRB of the two sources is a diagonal matrix containing the single-source CRBs for each of the sources on the diagonal. In other words, the two sources are completely decoupled, as if each of them was present alone. While the conditions for this case seem rather restrictive, it should be noted that this still is approximately true if the conditions are not exactly met (i.e., small residual correlation or almost maximum phase separation).

[1]The behavior of the CRB is symmetric in $\Delta\varphi$ since users can be exchanged and π-periodic since real-valued data streams can be multiplied by a factor of -1.

In Figure 1 we display the finite value $\mathrm{tr}\left\{\boldsymbol{C}^{(\mathrm{nc})}_{\lim}\right\}$. The top graph shows a 3d plot of $\mathrm{tr}\left\{\boldsymbol{C}^{(\mathrm{nc})}_{\lim}\right\}$ versus both, $\hat{\rho}$ and $\Delta\varphi$. The two graphs below display the behavior versus $\hat{\rho}$ for selected values of $\Delta\varphi$ and vice versa. We can see that $\mathrm{tr}\left\{\boldsymbol{C}^{(\mathrm{nc})}_{\lim}\right\}$ goes to infinity for $\hat{\rho} \to 1$ and $\Delta\varphi \to 0$. The behavior of $\mathrm{tr}\left\{\boldsymbol{C}^{(\mathrm{nc})}\right\}$ and $\mathrm{tr}\{\boldsymbol{C}\}$ for varying $\Delta\theta$ is shown in Figure 2. On the left hand side we see the trace of $\boldsymbol{C}^{(\mathrm{nc})}$, on the right hand side the trace of $\boldsymbol{C}$ for comparison. The four subplots represent four different values of $\hat{\rho}$: The top-left graph represents the uncorrelated case $\hat{\rho} = 0$ (leading to perfect decoupling for $\boldsymbol{C}^{(\mathrm{nc})}$), whereas the bottom-right graph shows full coherence. Note that in the case where $\Delta\theta \to 0$ the trace of $\boldsymbol{C}^{(\mathrm{nc})}$ reaches a finite value for $\Delta\varphi \neq 0$ and $\hat{\rho} < 1$ and the trace of $\boldsymbol{C}$ never reaches a finite value.

The decoupling result can be generalized to more than two sources in the following way: Suppose all the sources are perfectly uncorrelated, such that $\hat{\boldsymbol{R}}_{S,0}$ is a diagonal matrix. Additionally, the phase angles must fulfill the condition $\varphi_i = \varphi^{[1]} + k_i \cdot \pi$ **or** $\varphi_i = \varphi^{[2]} + k_i \cdot \pi$, for $k_i \in \mathbb{Z}$ and $i = 1, 2, \ldots, d$, i.e., modulo π there are only two different phase angles: $\varphi^{[1]}$ and $\varphi^{[2]}$ (corresponding to two distinct lines in the I/Q diagram). If then additionally $|\varphi^{[1]} - \varphi^{[2]}| = \pi/2$ then the joint CRB of all the sources decouples into two groups: All the users with phase $\varphi^{[1]}$ are completely decoupled from the users with phase $\varphi^{[2]}$ as if each of the groups was present alone. This results in a significant gain compared to the CRB for arbitrary source constellations if there are closely spaced sources that belong to different groups. Once again, this theorem is still approximately true if the strict conditions are not exactly fulfilled (e.g., small correlation).

Finally, another advantage non-circular sources are able to provide is in the total number of sources that can be estimated jointly. As an example, consider a uniform linear array with M sensors. In this case, $d = M - 1$ sources can be estimated jointly using arbitrary (non neccessarily strict sense non-circular) source constellations. Now it can be shown that for $\boldsymbol{C}^{(\mathrm{nc})}$ the number of sources can be as large as $d = 2(M - 1)$ as long as **none** of the sources are coherent (i.e., the sample correlation coefficients $\hat{\rho}_{i,j}$ all have a magnitude less than one for $i \neq j$) **and** the phase angles are all different modulo π: $\mathrm{mod}(\varphi_i, \pi) \neq \mathrm{mod}(\varphi_j, \pi) \;\forall i \neq j \in \{1, 2, \ldots, d\}$ (i.e., all the lines in the I/Q diagram are distinct). This has also been observed for the NC Unitary ESPRIT algorithm [5].

6. SIMULATION RESULTS

These features can also be demonstrated through computer simulations. Here, we compare the Unitary ESPRIT algorithm [4] and the corresponding deterministic CRB from (7) with the NC Unitary ESPRIT algorithm [5] and the CRB for strict sense non-circular sources from (8). As an example, consider Figure 3 where the separation of $d = 2$ uncorrelated sources is varied for an $M = 8$ sensor uniform linear array (ULA) using $N = 10$ subsequent snapshots. The SNR is set to 30 dB. We can clearly see how exploiting the strict sense non-circularity condition leads to a root mean square estimation error and a CRB that is constant as the two sources approach.

In Figure 4 the number of sensors is changed to 5 and the number

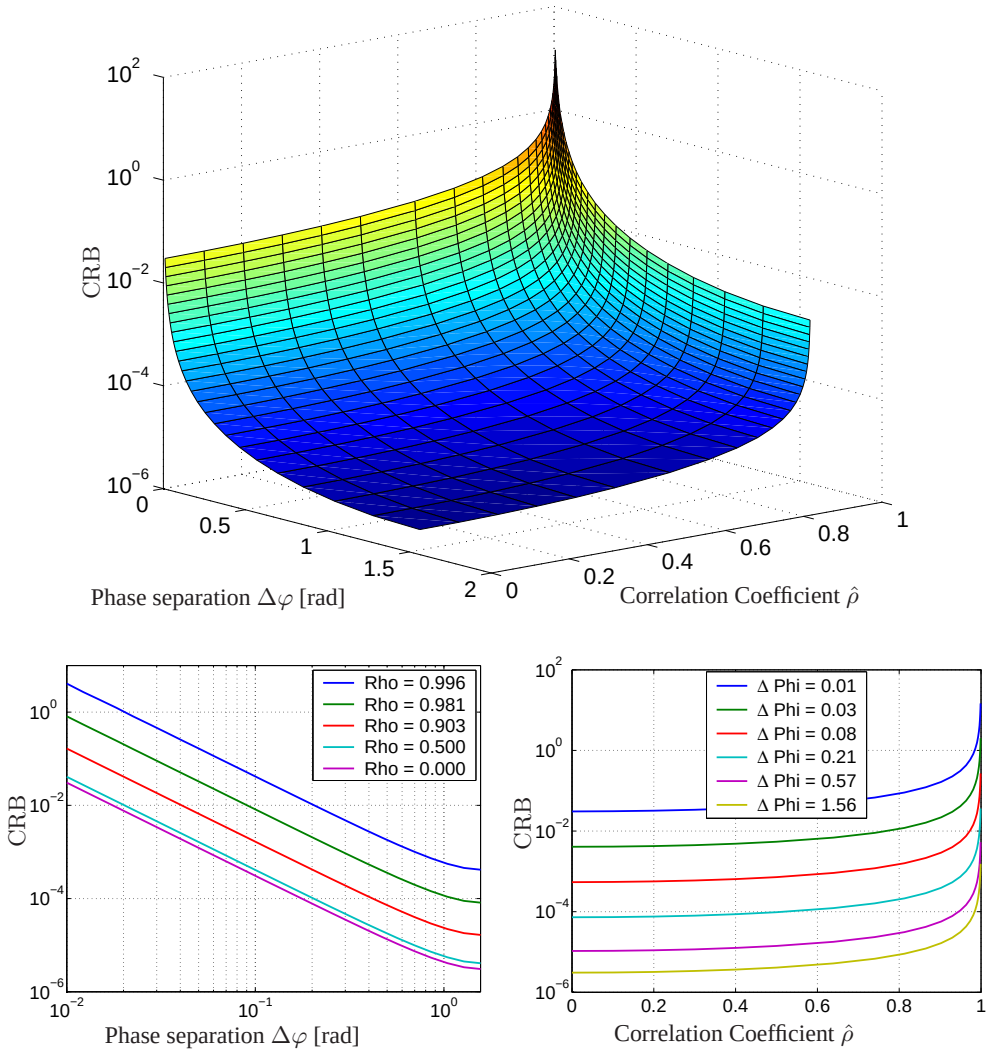

Fig. 1. Limit of the CRB for two sources and $\Delta\theta \to 0$ as a function of the correlation coefficient $\hat{\rho}$ and the phase separation $\Delta\varphi$.

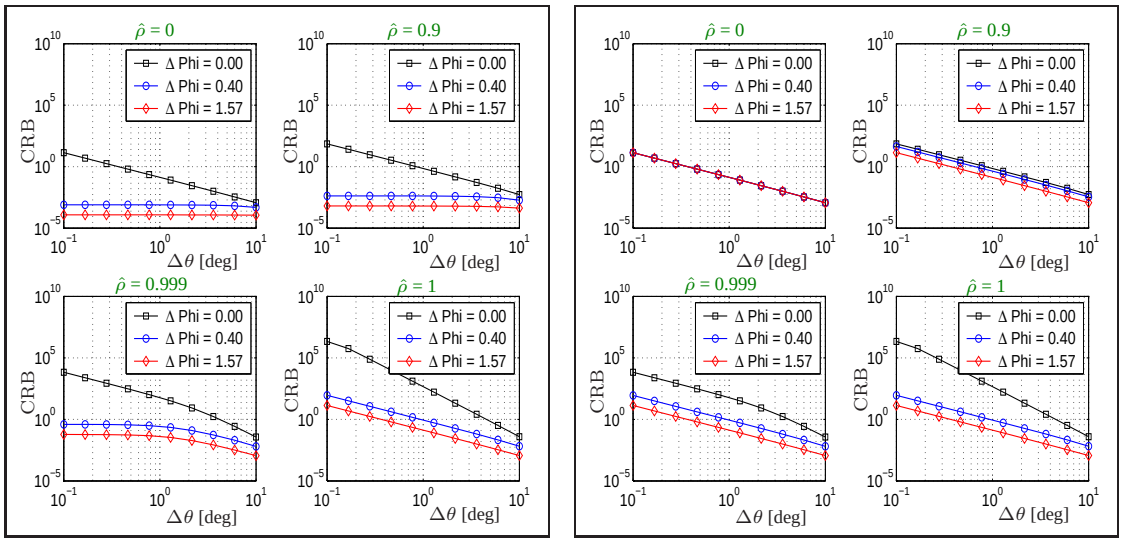

Fig. 2. CRB versus the separation of the two sources in the azimuth plane $\Delta\theta$. Left: trace of $\boldsymbol{C}^{(\mathrm{nc})}$, Right: trace of $\boldsymbol{C}$. The subplots represent different values for the correlation coefficient, i.e., $\hat{\rho} = 0, 0.9, 0.999, 1$ and in each graph different values for the phase separation are shown.

of sources is varied to demonstrate that the limit on the number of resolvable sources is doubled from $M-1$ to $2(M-1)$. The phase angles are drawn randomly according to a uniform distribution in $[0, 2\pi]$, the azimuth angles are set deterministically in the interval $[20^\circ, 160^\circ]$ with a fixed separation of 20°.

7. CONCLUSIONS

In this contribution, the Cramér-Rao Bound for strict sense non-circular sources is discussed. First, a closed form expression for the CRB for this data model is given. Then its behavior in some interesting special cases is studied. In particular, it is demonstrated that in the case where two sources approach the same position, a finite value for the CRB is reached. This implies a significant gain compared to arbitrary (i.e., not necessarily non-circular) source constellations where the CRB approaches infinity. The scenarios where the non-circular sources do not lead to any improvement in terms of the CRB are also outlined. The results are supported by computer simulations where the CRBs are compared with the corresponding versions of the Unitary ESPRIT algorithm.

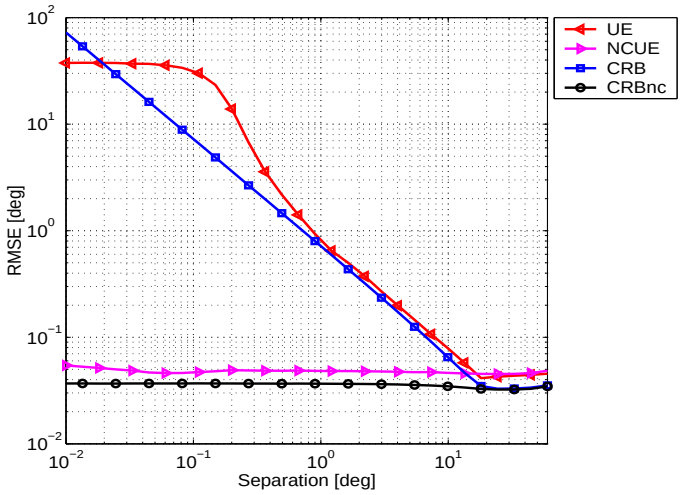

Fig. 3. Root mean square estimation error for Unitary ESPRIT (UE) and NC Unitary ESPRIT (NCUE) together with the corresponding CRBs versus the separation of $d = 2$ uncorrelated sources.

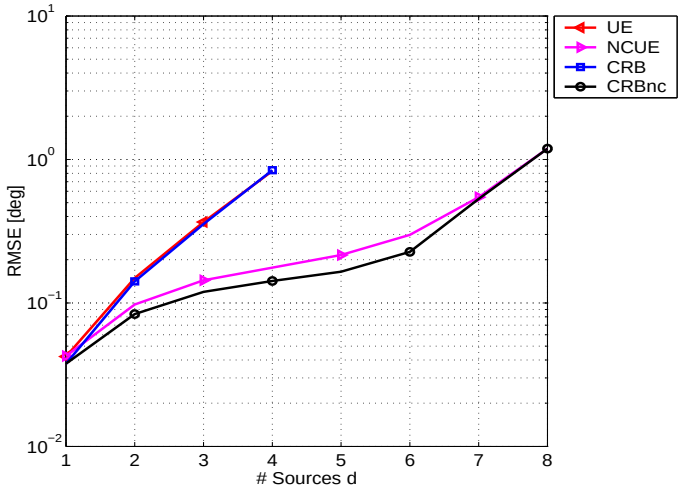

Fig. 4. Comparison of Unitary ESPRIT (UE) and NC Unitary ESPRIT (NCUE) versus the number of sources d for a 5 sensor ULA. The number of resolvable sources is doubled.

REFERENCES

[1] P. Chargé, Y. Wang, and J. Saillard. A root-MUSIC algorithm for non circular sources. In *Proc. International Conference on Acoustics, Speech and Signal Processing (ICASSP 2001)*, volume 5, pages 2985–2988, Salt Lake City, UT, May 2001.

[2] H. Cramér. *Mathematical Models of Statistics*. Princeton University Press, Princeton, New Jersey, 1946.

[3] J. P. Delmas and H. Abeida. Stochastic Cramér-Rao Bound for noncircular signals with application to DOA estimation. *IEEE Transactions on Signal Processing*, 52:3192–3199, November 2004.

[4] M. Haardt and J. A. Nossek. Structured least squares to improve the performance of ESPRIT-type high-resolution techniques. In *Proc. International Conference on Acoustics, Speech and Signal Processing (ICASSP 1996)*, volume V, pages 2805–2808, Atlanta, GA, May 1996.

[5] M. Haardt and F. Römer. Enhancements of Unitary ESPRIT for non-circular sources. In *Proc. International Conference on Acoustics, Speech and Signal Processing (ICASSP 2004)*, volume 2, pages 101–104, Montreal, Canada, May 2004.

[6] C. R. Rao. *Linear Statistical Inference and Its Applications*. Wiley, New York, 1946.

[7] F. Römer. Advances in subspace-based parameter estimation: Tensor-ESPRIT-type methods and non-circular sources. Diploma thesis, Ilmenau University of Technology, Communications Research Lab, October 2006.

[8] A. Salameh, N. Tayem, and H. M. Kwon. Improved 2-D Root MUSIC for Non-Circular Signals. In *Fourth IEEE Workshop on Sensor Array and Multichannel Processing*, pages 151–156, July 2006.

[9] P. Stoica and A. Nehorai. MUSIC, maximum likelihood, and Cramer-Rao bound. *IEEE Transactions on Acoustics, Speech, and Signal Processing*, 37:720–741, May 1989.

[10] P. Stoica and A. Nehorai. Performance study of conditional and unconditional direction-of-arrival estimation. *IEEE Transactions on Acoustics, Speech, and Signal Processing*, 38:1783–1795, October 1990.

[11] A. J. Weiss and B. Friedlander. On the Cramér-Rao Bound for direction finding of correlated signals. *IEEE Trans. Signal Process.*, SP-41:495–499, January 1993.

[12] A. Zoubir, P. Chargé, and Y. Wang. Non circular sources localization with ESPRIT. In *Proc. European Conference on Wireless Technology (ECWT 2003)*, Munich, Germany, October 2003.